



Cite this: *Environ. Sci.: Adv.*, 2022, 1, 47

## Synthesis and characterization of novel dual-capped Zn–urea nanofertilizers and application in nutrient delivery in wheat†

Christian O. Dimkpa,<sup>‡§\*a</sup> Maria G. N. Campos,<sup>‡§\*b</sup> Job Fugice,<sup>f</sup> Katherine Glass,<sup>f</sup> Ali Ozcan,<sup>beg</sup> Ziyang Huang,<sup>be</sup> Upendra Singh<sup>f</sup> and Swadeshmukul Santra<sup>‡bcde</sup>

Nanoscale nutrients are promising for improving crop performance. However, size-induced potential for drifting, segregation, or transformation warrants strategies to streamline fertilization regimes. Herein, we developed three nanofertilizers by coating urea granules with Zn nanoparticles capped with binary capping agents: *N*-acetyl cysteine (NAC) and sodium salicylate (SAL); NAC and urea; or SAL and urea. Coating was accomplished at 80–100% efficiencies. When evaluated in sorghum through soil application at 6.4 (rate-1) and 2.1 (rate-2) mg Zn per kg soil, the nanofertilizers influenced sorghum performance, plant accumulation, and soil retention of Zn, N, and P comparably with the control (Zn-sulfate). However, SAL–urea–Zn, NAC–SAL–Zn, and NAC–urea–Zn nanofertilizers evoked rate-dependent significant ( $P < 0.05$ ) effects compared to Zn-sulfate. Early SPAD (chlorophyll) counts were significant with SAL–urea–Zn rate-1, compared to Zn-sulfate. NAC–SAL–Zn and SAL–urea–Zn rate-1 significantly increased shoot biomass, compared to Zn-sulfate. Notably, NAC–urea–Zn rate-2 strongly promoted grain or total above-ground Zn or N accumulation compared to SAL–urea–Zn rate-1, NAC–SAL–Zn rate-1, or NAC–urea–Zn rate-1, indicating that a lower rate of Zn can be used for NAC–urea–Zn to facilitate Zn and N delivery. Residual soil Zn was significantly higher with NAC–SAL–Zn rate-1, compared to Zn-sulfate. However, residual ammonium was significantly higher in Zn-sulfate, compared to other treatments, except for NAC–urea–Zn rate-2. Contrarily, residual P was significantly higher with SAL–urea–Zn rate-1 than with Zn-sulfate. These findings indicate that coating of urea with Zn nanoparticles can facilitate the application of nanoscale nutrients in agriculture, without any penalty on plant performance or nutrient delivery.

Received 17th September 2021  
Accepted 7th January 2022

DOI: 10.1039/d1va00016k

rsc.li/esadvances

### Environmental significance

Nanoparticles are applied in agriculture as agrochemicals. However, use of nano-forms of trace nutrients like zinc is hampered by size-induced drift (and associated environmental/human health hazards), and particle segregation in bulk-fertilizer blends. There is, therefore, a need for strategies to deliver nanoscale micronutrients to plants. Also, the possibility of reducing nutrient application rates, thereby reducing the environmental footprint of chemical-fertilizers deserves exploration. We developed novel nano-enabled Zn-NP–urea fertilizers. The products showed comparable or better effects on plant performance, plant uptake or soil retention of nutrients than Zn-sulfate. Grain Zn fortification using a lower amount of Zn is especially important given widespread human Zn deficiency. This effect clearly demonstrates one of the goals of nano-enabled agriculture: reduction of nutrient input rates into the biosphere.

<sup>a</sup>Department of Analytical Chemistry, The Connecticut Agricultural Experiment Station, New Haven, Connecticut 06504, USA. E-mail: Christian.Dimkpa@ct.gov

<sup>b</sup>NanoScience Technology Center, University of Central Florida, Orlando, Florida 32816, USA. E-mail: nogueiracamposm@easternflorida.edu

<sup>c</sup>Department of Chemistry, University of Central Florida, Orlando, Florida 32816, USA

<sup>d</sup>Department of Materials Science and Engineering, University of Central Florida, Orlando, Florida 32816, USA

<sup>e</sup>Burnett School of Biomedical Sciences, University of Central Florida, Orlando, Florida 32816, USA

<sup>f</sup>Fertilizer Research Program, International Fertilizer Development Center, Muscle Shoals, Alabama 35662, USA

<sup>g</sup>Vocational School of Technical Sciences, Karamanoglu Mehmetbey University, Karaman 70200, Turkey

† Electronic supplementary information (ESI) available: Results of fast Fourier transform analysis and Fourier transform infrared spectroscopy. See DOI: 10.1039/d1va00016k

‡ Previous address: Fertilizer Research Program, International Fertilizer Development Center, Muscle Shoals, Alabama 35 662, United States.

§ Equal contribution.



## Introduction

Over-exploitation of renewable and non-renewable resources due to rising global population warrants alternative technologies to harness and deploy natural resources in a more sustainable manner. Among such resources, zinc (Zn) is used mostly in applications other than agriculture.<sup>1</sup> However, Zn is a critically important crop nutrient often co-lacking in soils, crops, and humans globally, due to a strong interlinkage in the soil–crop–human continuum.<sup>2,3</sup> Notably, global Zn resources are not infinite; estimates indicate that their depletion could happen in less than 25 years.<sup>1</sup> Conventionally, Zn fertilizer is applied to crops mainly in the form of salts, particularly zinc-sulfate (ZnSO<sub>4</sub>). Other forms of Zn used in agriculture include bulk-scale ( $\geq 1000$  nm) zinc oxide (ZnO) powder, and chelated Zn such as Zn-EDTA (ethylenediaminetetraacetic acid), Zn-EDDHA [ethylenediamine-*N,N'*-bis(2-hydroxyphenylacetic acid)] and Zn-lignosulfonate.<sup>4</sup> In contrast to these Zn forms, the advent of nanotechnology has permitted the development of novel Zn types based on the particle size, with markedly different reactivities and bioenvironmental responses.<sup>5–8</sup> Notably, zinc oxide nanoparticles (ZnO-NPs;  $\leq 100$  nm in at least one dimension) are incorporated into a variety of industrial, medical, and household products, to enhance the quality and functionality of Zn.<sup>9</sup> These NPs are increasingly being explored as fertilizers and pesticides to harness their novel properties in maximizing crop productivity.<sup>5,7,10–13</sup>

The increasing number of studies show that Zn-based NPs can enhance plant performance when used at judicious application rates.<sup>5–8</sup> However, such benefits are still far from being maximized for large field-scale crop production due to the inherent and practical problems associated with micronutrients needed by plants in trace amounts, which are further complicated by the ultra-small size of nanoscale nutrients. As previously discussed,<sup>6</sup> whereas a conventional fertilizer can be applied by surface broadcast, the inherency of nanoparticles to suspend in air would lead to drift losses, negating the applicability of surface broadcast with dry ZnO-NPs. Moreover, drifting of nanoscale materials can potentially result in exposure of the handler and other unintended biological targets to the materials. On the other hand, whereas deep placement of the nanopowder into the soil can eliminate drift hazards, nanoparticle adhesion to equipment surfaces, especially under wet conditions, could alter the form and function of the nanofertilizer product. Similarly, suspensions of nanoparticles in water, especially of non-surface modified products, for use as soil drench, foliar spray, or fertigation can also be problematic. In aqueous environments, pristine nanoparticles either dissolve into ions or aggregate into non-nanoscale structures. Particle dissolution obfuscates the effect of the nanofertilizer treatment owing to the prevalence of ionic activity.<sup>14,15</sup> Similarly, aggregation of nanoparticles negates the definition of “nano” and associated size-specific reactivity. Both scenarios essentially counteract the underlying functionality of the nanofertilizer.

From a practical standpoint, there is a large mass difference between macronutrient fertilizers, such as NPK granules (2–

4 mm size), and conventional Zn fertilizer particles ( $\mu\text{m}$  size). Such difference causes size-dependent particle segregation when nutrients are blended and packaged. Given the smaller size of nanoscale materials, it is highly likely that particle segregation will exacerbate when using nanoscale ZnO for blending with macronutrient granules. Furthermore, large-scale field application of micronutrients such as Zn that are required in small amounts is known to result in non-uniform distribution of the nutrients, leading to sporadic and unpredictable effects on crop productivity.<sup>16</sup>

Considering the above-mentioned issues, it is critical to develop strategies for delivering nano-scale nutrients to plants that are both effective and safe, and that simultaneously accommodate size differences in fertilizer-nutrient particles. One strategy that is starting to be explored in this regard is the physical incorporation of a nanopowder and a macronutrient fertilizer such as urea or NPK granules<sup>17–20</sup> to generate so called “nano-enabled” fertilizers, defined as conventional fertilizers having one or more nanoscale components or additives.<sup>6,8,21</sup> Previous studies reported doping or coating urea with ZnO-NPs.<sup>5,17,18</sup> Such coatings involved using facile systems that involved water or vegetable oil as a binding agent. We hypothesized that dual capping of Zn NPs prior to coating of fertilizer granules would further improve product efficiency through increasing the dispersibility of Zn, as well as controlling the particle size to obtain ultra-small particles ( $\sim 5$  nm). Therefore, in the present study we have developed a novel nano-enabled fertilizer composed of urea and Zn involving coating of urea with dual-capped Zn-NPs. In the formulation, the Zn NPs were first capped with binary combinations of *N*-acetyl cysteine (NAC), sodium salicylate (SAL), and urea, before being coated onto urea granules. The present study deals with the efficiency of nanofertilizers in enhancing plant performance and nutrient delivery, in comparison with the gold standard Zn fertilizer, ZnSO<sub>4</sub>.

## Materials and methods

### Synthesis of dual-capped Zn-NPs

In this work, Zn-NPs, rather than ZnO NPs were synthesized at room temperature using a wet chemical precipitation method following a published protocol,<sup>22</sup> with slight modification to accommodate two surface capping agents. Briefly, 91 g zinc nitrate hexahydrate was dissolved in 700 mL DI water and the two capping agents (NAC–SAL: 12.5 g NAC and 12.2 g SAL; NAC–urea: 12.5 g NAC and 4.6 g urea; or SAL–urea: 12.2 g SAL and 4.6 g urea) in powder form were added directly to the solution under stirring.

Dual-capping was conducted to enhance the stability of the nano Zn for use in urea coating. In addition to being a stabilizer, NAC is an antioxidant that modulates plant response to biotic and abiotic stresses,<sup>23–25</sup> and has been previously used to cap ZnO NPs, with a strong stabilization outcome for the NPs (reviewed in 7). In terms of application as an agrochemical, the co-application of NAC and Zn or Cu has been reported to increase metal availability to plants,<sup>26,27</sup> while the formulation of NAC with ZnO and albumin demonstrated antimicrobial



activity against *candidatus Liberibacter asiaticus* (cLas) in citrus.<sup>22</sup> On the other hand, SAL, a plant-derived hormone, plays a role in plant growth and development.<sup>28</sup> Notably, the co-application of SAL and Zn improved plant performance under water stress<sup>29</sup> as well as under prolonged low temperature exposure.<sup>30</sup> Therefore, we suppose that use of these stabilizers in the synthesis of Zn NPs could produce interesting surface properties that can be leveraged to coat urea, in addition to potential beneficial effects in plants.

During stirring, the pH was slowly raised to 9 by dropwise addition of 1 M NaOH<sub>(aq)</sub> solution, under vigorous stirring using a mechanical stirrer (800 rpm). The final volume was adjusted to 1 L, and the solution was left stirring overnight. In all cases, the final metallic Zn concentration was 20 000 ppm (mg L<sup>-1</sup>). For subsequent characterization (except for DLS and zeta potential measurements), the Zn-NP aqueous suspension was centrifuged at 10 000 rpm for 5 min (Eppendorf Centrifuge 5810R, 15amp version). The Zn-NP pellet was then lyophilized (FreeZone® 4.5 Liter Freeze Dry Systems Model# 7750020) to obtain solid powder.

### Characterization of dual-capped Zn NPs

The dual-capped Zn-NPs were characterized by zeta potential, dynamic light scattering (DLS), atomic absorption spectroscopy (AAS), infrared spectroscopy (FTIR), X-ray diffraction (XRD), and high-resolution transmission electron microscopy with fast Fourier transform (HR-TEM/FFT) analysis. For DLS and zeta potential, the 'as-synthesized' dual-capped Zn-NP suspensions were diluted in DI water and analyzed for hydrodynamic particle size and surface charge using a Malvern Zetasizer (model Nano ZS90). AAS was done using a Perkin Elmer Analyst 400 spectrometer to determine the Zn content of the NP suspension. For the AAS sample preparation, 10 mg lyophilized powder of each dual-capped Zn-NP formulation was digested using 10 mL of an aqueous solution of 1% HCl in a 15 mL disposable centrifuge tube. A PerkinElmer Spectrum 100 Series Infrared Spectrometer was used for FTIR measurements. The scan was focused to identify any peak associated with the zinc-oxygen interaction in addition to other characteristic FTIR peaks of urea, SAL and NAC. The crystalline pattern of the lyophilized powder was studied by X-ray diffraction (PANalytical Empyrean, model number). For HR-TEM/FFT, the lyophilized powders were re-suspended in DI water to obtain the Zn-NP suspension (1 mg mL<sup>-1</sup>). The NP suspension was sonicated using an ultrasonicator (Elmasonic S 30 H) prior to drop-casting on a TEM grid (Electron Microscopy Sciences, CF300-AU-UL). The grid was then air-dried overnight. HR-TEM analysis was performed on a FEI Tecnai F30 Transmission Electron Microscope. Fast Fourier Transform (FFT) analysis was performed and the results were compared with those of wulffingite zinc hydroxide.

### Coating of urea granules with dual-capped Zn NPs

The nanofertilizers used in this study were developed by coating urea granules with the dual-capped Zn-NPs. To this end, commercially obtained urea granules were sieved to between 1.7 and 4 mm particle sizes and approximately 0.5 kg of urea was

loaded into a batch, laboratory-scale, fluidized bed unit (UNI Glatt, Norwood, NY, USA) having a cylindrical receptacle, with an inner cylinder with a spray nozzle directed upward. A suspension of each dual-capped Zn-NP formulation, dilute enough to allow for spraying, was first colored using water-soluble food-grade dye (McCormick, Hunt Valley, Maryland) to enable contrasting between each formulation and urea granules, both of which are white in color. Subsequently, the nanosuspensions were pumped at a rate of 1–3 mL min<sup>-1</sup> to the fluidized bed nozzle *via* a peristaltic pump and atomized with compressed air. The granular urea was coated using a layering technique. Approximately 200 mL of the Zn-NP suspension was sprayed repeatedly until the desired Zn concentrations of 1 and 3% Zn were reached. This process was conducted for each of the products. Separately, plain urea was coated with the same food-grade dye as a control. These food grade dyes had been used in the past and shown to have no effect on crops.<sup>19</sup>

### Characterization of dual-capped Zn NPs-urea nanofertilizers

Upon coating, a representative sample of each product was analyzed for Zn content by acid digestion (20 mL of 50% HCl), followed by boiling for 15 min, filtration and dilution, and using an Inductively Coupled Plasma Optical Emission Spectrometer (ICP-OES; Spectro Arcos, SPECTRO Analytical Instruments GmbH, Kleve, Germany). Furthermore, each product was morphologically characterized by scanning electron microscopy (Zeiss ULTRA-55 FEG SEM). To this end, the coated granules were placed in a desiccator for 24 h and then carefully sliced with a razor blade for cross-sectional imaging. EDS spectra of the core and the shell parts were recorded.

### Soil preparation and plant growth

A sandy loam soil (pH, 6.87; organic matter content, 0.92%; N : P : K, 4.0 : 2.05 : 246.0 mg kg<sup>-1</sup>, and [DTPA-extractable] Zn level, 0.1 mg kg<sup>-1</sup>, indicating a Zn deficiency status)<sup>31</sup> was used in a pot experiment conducted under greenhouse conditions at the International Fertilizer Development Center (IFDC) in Muscle Shoals, Alabama, to evaluate the effects of the nanofertilizers on plant performance and delivery of Zn, nitrogen (N) and phosphorus (P) to plants. Treatments were randomly assigned using a block design that comprised three replications per treatment. To this end, pots (≈ 162 cm<sup>2</sup>) were loaded with 7 kg of soil, and basal P and potassium (K) were added at 75 mg kg<sup>-1</sup> and 50 mg kg<sup>-1</sup>, respectively, by mixing into the soil using a rotary shaker. The sources of P and K were monocalcium phosphate and potassium sulfate, respectively. Four seeds of *Sorghum bicolor* (variety 251) were planted 2 cm deep in each potted soil. On week post germination, seedlings were thinned down to 1 per pot. Subsequently, the urea-Zn nanofertilizer experimental treatments were surface-applied 2 weeks after germination by placing the coated urea granules on the soil, 2 cm away from the plants. For the control Zn treatment, the appropriate amount of Zn-sulfate (as a heptahydrate salt; ZnSO<sub>4</sub>·7H<sub>2</sub>O) corresponding to 3% Zn was added. This control Zn was physically separated from the urea but placed in the same general vicinity on the soil. The control urea was coated



with food-grade dye but lacked the presence of Zn on it. The following 6 treatments were established: control (urea with separate application of ZnSO<sub>4</sub>); NAC-SAL-Zn, rate 1 (6.4 mg Zn per kg soil) and rate 2 (2.1 mg Zn per kg soil); SAL-urea-Zn rate-1; and NAC-urea-Zn, rates 1 and 2. The rate-1 products represented urea coated with Zn at 3% of the granule weight, and the rate-2 products represented granules coated with Zn at 1% by weight. Due to differential efficiencies of coating urea with the dual-capped Zn-NP, the %, and thus, Zn concentration of the Zn-coated products varied slightly among the products. The pre-application product Zn concentrations for the 3% products amounted to 7.7 mg kg<sup>-1</sup> soil for NAC-SAL, 6.4 mg kg<sup>-1</sup> for NAC-urea, and 6.4 mg kg<sup>-1</sup> for SAL-urea. The Zn application rate was, therefore, normalized to 6.4 mg kg<sup>-1</sup> soil by reducing the amount of coated granular urea used in the NAC-SAL-Zn treatment application to 1.26 g and replacing the urea with the control urea to, again, achieve 1.5 g urea per pot (100 mg N per kg soil) for all treatments. The normalized Zn application concentration for the 1% (rate-2) coating was, thus, 2.1 mg kg<sup>-1</sup>.

Top-dressing with N was performed at around V6-V8 stages of vegetative development, whereby 0.75 g of control urea amounting to 50 mg N per kg soil was supplemented in each pot. Watering and other management practices for all treatments followed standard greenhouse plant growth procedures. During plant growth, data were collected on chlorophyll content using a SPAD Meter (Soil-Plant Analyses Development) meter (Konica Minolta). Standard SPAD measurement consisted of placing an intact plant leaf in between the meter and recording the values indicated. Three leaves were measured from different positions in a plant and averaged, to generate a SPAD reading for each plant. At full physiological maturity, plants were harvested, separated into straw (stems, leaves and panicle head) and grains. These tissues were then dried at ~60 °C to determine the dry-matter yield. Subsequently, straw and grains were ground separately and analyzed for shoot nutrient uptake or grain nutrient translocation, respectively. Ground plant tissues were acid-digested in a solution of sulfuric acid (3 mL) and hydrogen peroxide (1 mL), heated for one h at 350 °C, cooled to ambient temperature, and then equilibrated with dd-H<sub>2</sub>O. A skalar segmented flow analysis was used to determine the N and P contents in the samples, while inductively coupled plasma-optical electron spectroscopy (ICP-OES) was used for measuring the Zn content. In addition, soil samples were also collected post-harvest for each treatment, to determine available residual levels of N (in the forms of nitrate and ammonium), P and Zn. To this end, soil samples in replicates were ground and sieved, followed by extraction using KCl for ammonium and nitrate-N; for P by using an iron oxide-

impregnated filter paper (the Pi method;<sup>32</sup>); and for Zn by DTPA (1 : 2 w/v [soil : DTPA solution]). All soil samples were shaken for 2 h and filtered before being subjected to analytical measurements using the respective instruments used for the plant tissues.

### Data analysis

A one-way analysis of variance (ANOVA; OriginPro 2018) was used to determine significant differences in crop responses to the treatments. A Fisher LSD means comparison was performed to further explore the differences with significant ( $p \leq 0.05$ ) ANOVA.

## Results and discussion

Herein we report a novel nano strategy for Zn delivery in agricultural plants. Previous studies directly used ZnO NPs for coating on urea. The current study is novel in its use of dual-capped Zn-NPs to enhance the stability of the nano Zn for use in urea coating. The results of this approach and effects on wheat performance are presented below.

### Characterization of dual-capped Zn NPs

The surfaces of the NAC-SAL Zn-NP and NAC-urea Zn-NP suspensions were negatively charged, with similar zeta potential values (Table 1). The negative charge can be attributed to the carboxylic group of NAC that is in the anionic form at pH 9.0 ( $pK_a = 3.24$ ).<sup>33</sup> That contrasted with the positive zeta potential of the SAL-urea Zn-NP formulation (Table 1), which can be attributed to the lower prevalence of negative charge in SAL being suppressed by the higher prevalence of positive charge in urea, rendering a net positive charge. DLS analysis indicated an average hydrodynamic size range of 125 nm for the Zn-NP formulations (Table 1), suggesting low colloidal stability caused by the lower surface charges ( $-30 \text{ mV} < \text{zeta potential} < +30 \text{ mV}$ ). However, this finding also indicated that dual capping minimally increased the particle size from the conventional theoretical 100 nm definition of nanoscale materials (Table 1). Subsequent analysis of the metal content following acid-digestion of the lyophilized powder of each dual-capped Zn-NP formulation indicated that the Zn content was around 20% in all three formulations (Table 1).

The negative surface charge observed with two of the suspensions at pH 9 was lower than that previously reported for ZnO-NPs,  $-24 \text{ mV}$ , in dd water suspension at pH 7.<sup>34,35</sup> However, both positive and negative surface charges have been reported for ZnO-NPs at pH 9, and are dependent on the presence of

**Table 1** Particle size, surface charge and Zn contents of dual-capped Zn nanoparticles

Product	Average hydrodynamic diameter (nm)	Zeta potential (mV; pH = 9.0)	Zinc content (% w/w)
NAC-SAL Zn-NP	116 ± 27	-17 ± 6.7	18 ± 2.8
NAC-urea Zn-NP	123 ± 25	-16 ± 8.4	19 ± 1.8
SAL-urea Zn-NP	135 ± 32	+28 ± 3.5	22 ± 1.9



additives and their interactions.<sup>36</sup> Thus, the overall data on surface charge for the Zn-NPs were not surprising. Generally, colloidal suspensions with high negative or positive zeta potential are considered stable.<sup>37–39</sup> The zeta potentials recorded with the formulations appear to be high enough to maintain their stability, as supported by the HR-TEM data (see below). Although the DLS data would suggest that the particle sizes are above 100 nm, DLS and microscopy data are known to often show inherent divergence in their estimation of particle size due to solution chemistry effects that modulate the particle hydrodynamic size but are absent in microscopic analysis.<sup>38</sup>

To investigate the interactions among the capping agents and Zn-NPs, FTIR spectra were analyzed, and the peaks were compared to those of the respective capping agents. ESI (Table SI 1†) shows the main peaks identified by FTIR for the dual-capped Zn-NP formulations. Due to the presence of multiple components in the system, some of the peaks overlapped, but the main peaks were identified (Table SI 1†). As indicated, for the NAC containing samples, namely, NAC–SAL Zn-NPs and NAC–urea Zn-NPs, main peaks were found for N–H bending around 1600  $\text{cm}^{-1}$  and O–H around 1350  $\text{cm}^{-1}$ . However, the peak at around 2550  $\text{cm}^{-1}$ , characteristic of the S–H bond,<sup>40</sup> was not found in both NAC–SAL Zn-NP and NAC–urea Zn-NP spectra. This may suggest that NAC interacts with Zn-NPs through the sulfur bond, although the band at around 1600  $\text{cm}^{-1}$  can also be attributed to Zn-carboxylic acid.<sup>41</sup> Comparing the SAL-containing formulations, namely NAC–SAL Zn-NPs and SAL–urea Zn-NPs, several peaks attributed to the aromatic compound not found for NAC–urea Zn-NPs were identified, including a C=C stretch around 1450 and 1490  $\text{cm}^{-1}$  and C–H bending peaks between 700 and 820  $\text{cm}^{-1}$ . Moreover, a peak indicating the Zn-carboxylate interaction was found at 1596  $\text{cm}^{-1}$  and 1603  $\text{cm}^{-1}$  for NAC–SAL Zn-NPs and SAL–urea Zn-NPs, respectively. Rawal *et al.*<sup>41</sup> reported that salicylate strongly interacts with Zn NPs *via* the formation of oxygen–zinc bonds in a coordination ring structure. Notably, comparing NAC–urea Zn-NPs and SAL–urea Zn-NPs, the characteristic bands of N–H stretching in the amine group were only observed in the SAL–urea Zn-NP spectrum, while a shoulder was found for NAC–urea in the same region.

ESI (Fig. SI 1 and SI 2†) shows the spectra of the capping agents only, and for the dual capped Zn-NPs, respectively. Similar to a previous report,<sup>40</sup> NAC showed main absorption peaks characteristic of carboxylic acid (1711  $\text{cm}^{-1}$ ), amide II at 1533  $\text{cm}^{-1}$  and the N–H stretching band at 3376  $\text{cm}^{-1}$ ; as well as of the S–H stretching bond (2548  $\text{cm}^{-1}$ ), as previously demonstrated (Fig. SI 1†). For urea, which has a simpler structure than NAC, the peaks of the N–H stretching in amine groups were identified at 3320 and 3430  $\text{cm}^{-1}$ . The N–H bond deformation peak was found at 1598  $\text{cm}^{-1}$ , and the stretching frequency of C–N was found at 1462  $\text{cm}^{-1}$ , followed by the stretching peak for C=O at 1676  $\text{cm}^{-1}$ , in agreement with prior data.<sup>42</sup> SAL exhibited the most complex structure among the capping agents, showing multiple peaks, including those characteristic for aromatic compounds, such as C–H bending (all peaks from 680 to 900  $\text{cm}^{-1}$ ), C=C stretching (1466 and 1620  $\text{cm}^{-1}$ ), and phenyl (739 and 1141  $\text{cm}^{-1}$ ). In addition, the C=O stretching band at 1647 and the benzene fingerprint peak at 1910  $\text{cm}^{-1}$  were identified as previously observed.<sup>43</sup> The  $\text{p}K_{\text{a}}$  for the thiol group is 9.52; as such, part of the sulfur is expected as the thiolate anion at pH 9.0.<sup>44</sup> However, as indicated in Fig. SI 2, a thiol peak was not found for both NAC–SAL and NAC–urea Zn-NPs, suggesting that the NAC-thiol group interacts with Zn-NPs. In contrast, the positively charged SAL–urea Zn-NPs have a higher modulus in comparison to NAC–SAL and NAC–urea Zn-NPs. As a consequence of the interaction of urea with Zn, the amine group becomes protonated as the NCO group assumes its polar resonance form, causing an increase in the frequency of the CN bond. This was observed in the FTIR spectrum (Fig. SI 2†) where two peaks in the amine N–H stretching region were present around 3300–3500  $\text{cm}^{-1}$ .<sup>45</sup> Notably, given the higher surface charge, the SAL–urea Zn-NP suspension was more stable in aqueous suspension than the NAC–urea and NAC–SAL Zn-NPs, which resulted in a more uniform coating of urea granules by this formulation.

XRD analysis of the formulations is shown in Fig. 1. The SAL–urea Zn-NP formulation presented more defined and intense peaks, compared to the NAC–SAL and NAC–urea Zn-NP formulations. However, in all cases, the peaks did not match ZnO or  $\text{Zn}(\text{OH})_2$  XRD diffraction peaks. This can be due to the

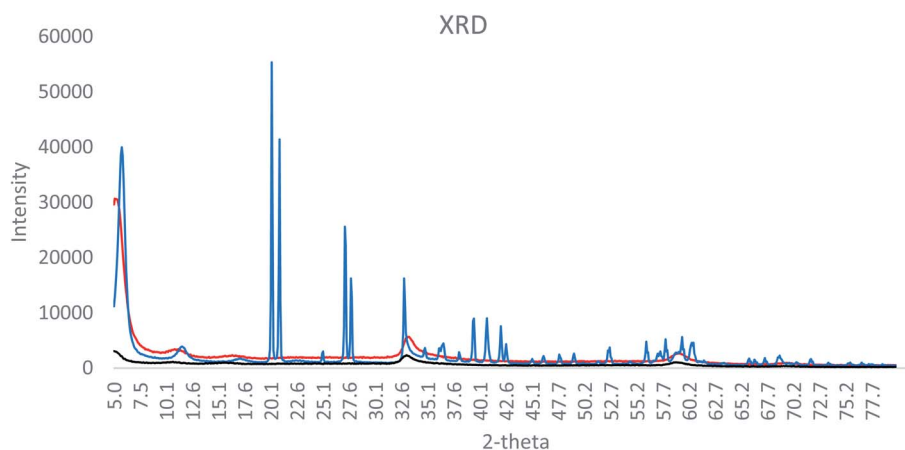


Fig. 1 X-ray diffraction pattern of (black) NAC–urea Zn NP, (blue) SAL–urea Zn NP and (red) NAC–SAL Zn NP.



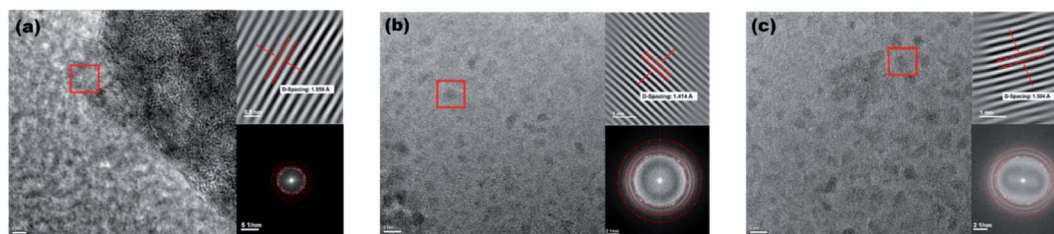


Fig. 2 HR-TEM images for (a) NAC-urea Zn NPs, (b) SAL-urea Zn NPs, and (c) NAC-SAL Zn NPs.

complex nature of the composition of the formulations, which may obfuscate the crystalline structure. As XRD analysis was inconclusive, HR-TEM Fast Fourier Transform (FFT) analysis was performed (Fig. 2), showing an individual particle size of around 5 nm in all three formulations. Based on the crystal lattice distances ( $d$ -spacing) from HR-TEM, it was possible to match the crystalline structure of the samples with wulffingite zinc hydroxide (Table SI 2<sup>†</sup>). Accordingly, the nanoparticles can be described more appropriately as Zn-NPs, rather than as ZnO-NPs.

### Morphological studies on dual-capped Zn NP-urea nanofertilizers

Visual observation of the coated urea indicated that coating urea with the SAL-urea Zn-NP formulation resulted in more homogeneous distribution of the coat around the urea granules than with the other formulations. In contrast, the NAC-SAL and NAC-urea Zn-NPs showed a “popcorn” like coating (Fig. 3). However, when preparing samples for SEM, the SAL-urea coating (shell) was more susceptible to segregation from the core (urea granule) after cross-sectioning. This suggested NAC-urea and NAC-SAL Zn-NP coatings adhered more strongly to the surface of the urea granules, probably due to the negative charges of these formulations. In this regard, although pure urea is as a neutral molecule, its processing into a granular commercial fertilizer involves the inclusion of additives such as anticaking agents, some of which are cationic,<sup>46,47</sup> and hence, could alter the urea surface properties thereby modulating interactions when used in subsequent formulations. In addition, the greater adhesion of NAC-SAL and NAC-urea Zn-NPs to the granules could also be due to the amorphous nature of these coatings as well as due to their topography which increases the interfacial surface area between the core and shell.

Scanning electron microscopy shows the core-shell structure of the urea granules coated with the dual-capped Zn-NPs



Fig. 3 (Left to right): Photo of control urea, NAC-SAL Zn NP-coated urea granules, NAC-urea Zn NP-coated urea granules, and SAL-urea Zn NP-coated urea granules.

(Fig. 2). Thus, these formulations could be successfully coated onto urea granules, produced in the case of the NAC-urea and NAC-SAL Zn-NP structures that were similar to previously observed.<sup>18</sup> The higher crystallinity of SAL-urea Zn-NPs observed by XRD was confirmed by SEM. Rod-shaped crystals can be found in the zoom image of this coating (Fig. 4, bottom left). These crystals were not present in the NAC-SAL and NAC-urea Zn-NP coated granules, which showed an amorphous structure (Fig. 4, top right zoom and bottom left zoom, respectively). As with the SAL-urea Zn-NP product, granules with high crystallinity and needle-like shapes were also observed with urea coated with ZnO in a previous study in which a mixture of honeybee wax and gallic acid was used as a binder.<sup>48</sup> This suggests a potential role for organic acid constituents in the process. Notably, such shapes were absent in the granules coated with NAC-containing formulations, suggesting that the related mechanism may have been altered by the presence of NAC. Elemental analysis was performed by EDS in cross-sectioned granules to assess the presence of Zn in the core and shell. The average Zn weight percentages on the shell of the coated granules were comparable,  $26.6 \pm 2.2$ ,  $25.5 \pm 2.2$  and  $22.6 \pm 0.2$ , respectively, for the NAC-SAL Zn-NP, NAC-urea Zn-NP, and SAL-urea Zn-NP coatings. No zinc was found in the control granules (urea only), as well as in the core of the Zn-coated granules. Fig. 3 further shows the SEM images as EDS peaks for the outer surface of the granules. As expected, peaks for carbon, oxygen and nitrogen were observed in the control granules. All dual-capped Zn-NP coated granules showed a peak for Zn in addition to peaks present in the control granule. The NAC-SAL and NAC-urea-Zn-NP-coated granules also showed sulfur peak due to the NAC chemical composition. The peak for Na found in all Zn-coated granules can be attributed to the NaOH used during the nanoparticle synthesis. The peak for gold is due to the sample sputter coating.

### Coating efficiencies of dual-capped Zn NP-urea nanofertilizers

The Zn contents of the coated urea granules by weight are 3.5 and 0.9%; 2.9 and 0.8%; and 2.9 and 1.0%, for NAC-SAL Zn, rate-1 and rate-2; NAC-urea Zn, rate-1 and 2; and SAL-urea Zn, rate-1 and rate-2, respectively. Specifically, the NAC-SAL Zn, rate-1 product contained a Zn amount that was higher than the targeted Zn rate of 3%. Typically, coating losses can occur during fertilizer production that involves surface coating.<sup>19</sup> The NAC-SAL Zn at rate-1 showed less coating loss, resulting in



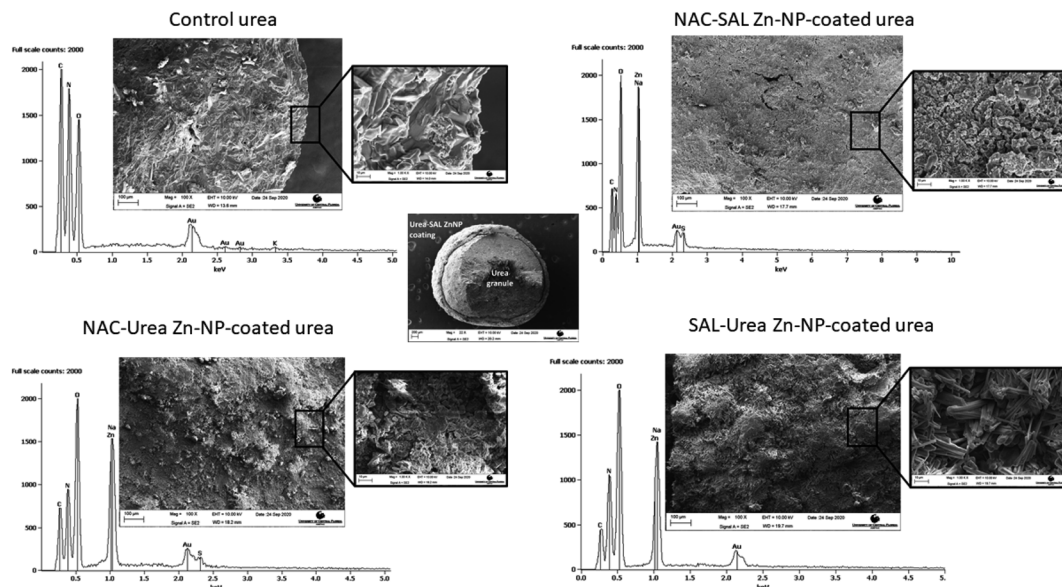


Fig. 4 SEM images and EDS spectra of control urea granule, and of NAC–SAL, NAC–urea and SAL–urea Zn NP coated urea granules. Middle inset is a representative cross-section of the Zn-NP coated urea, in this case, SAL–urea, showing the core and the coated shell.

a higher % Zn content. The coating process was considered efficient, overall. Efficiency is defined here as the ratio of Zn in the products to the initial target amount of Zn used for coating each product [3 and 1%, respectively, for rate-1 and rate-2] expressed as a percentage. The efficiencies were 100% and 90% for NAC–SAL Zn rate-1 and rate-2. They were 97% and 80% for NAC–urea Zn, rates-1 and 2. And they were 97% and 100% for SAL–urea Zn rate-1 and rate-2. Thus, coating efficiency was highest with the NAC–SAL Zn rate-1 and SAL–urea Zn rate-2 products, and lowest with the NAC–urea Zn rate-2 product.

These high efficiencies demonstrate the effectiveness of the fluidized bed coating process used in the present study.

#### Effect of Zn NP–urea nanofertilizers on the agronomic performance of sorghum

SPAD count, a measure of the chlorophyll content of plants, was promoted by all the Zn-NP–urea nanofertilizers during early vegetative growth (25 days after treatment; DAT), when compared to the ionic Zn control. The values were significant ( $P$

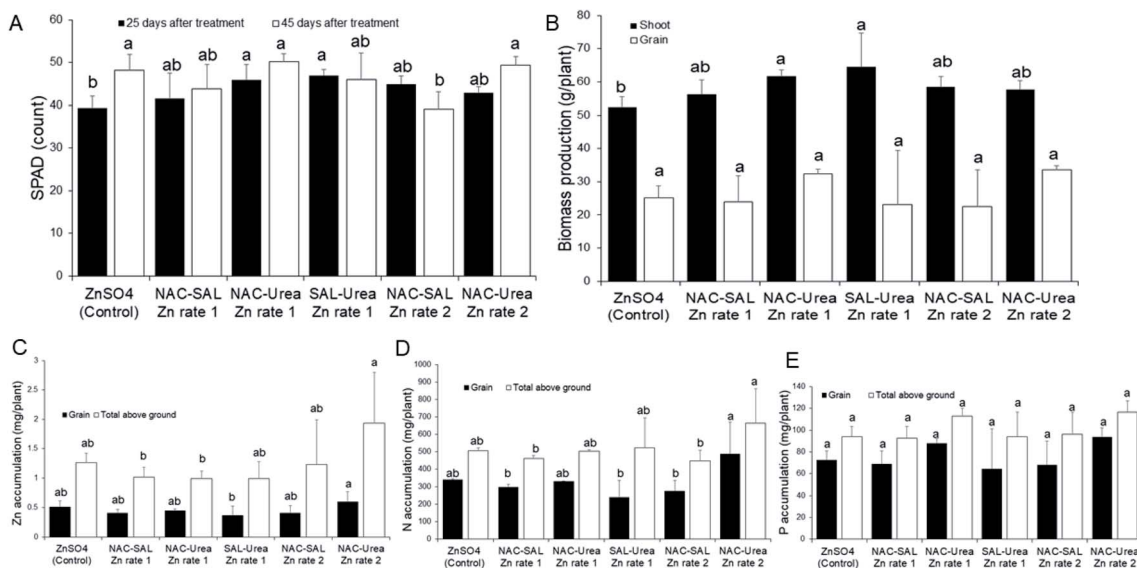


Fig. 5 Effects of Zn–urea nanofertilizers on chlorophyll content (SPAD count) (A), and biomass (grain and shoot) production (B) in sorghum; and accumulation of zinc (C); nitrogen (D), and phosphorus (E) in sorghum. Separately for SPAD count and biomass (shoot or grain, differently analyzed) production, bars followed by different letters are significantly different at  $P < 0.05$  ( $n = 3$ ). Separately for Zn, N and P (and in each case, for grain and total accumulation of each nutrient), bars followed by different letters are significantly different at  $P < 0.05$  ( $n = 3$ ).



< 0.05) with the SAL-urea-Zn rate-1 product, whereas other products resulted in median values, relative to SAL-urea-Zn rate-1 and the control treatments (Fig. 5A). In contrast, all treatments evoked a similar effect on SPAD counts at the later development stage (45 DAT), except for the NAC-SAL-Zn rate-2 treatment where the SPAD value was significantly lower (Fig. 5A). These SPAD values agree with those previously observed in sorghum exposed to ZnO NPs when provided separately from NPK fertilizer.<sup>49</sup> Indeed, as with SPAD data at 25 DAT, Subbaiah *et al.*<sup>50</sup> also observed uncapped ZnO NPs to increase SPAD levels in maize plants, relative to Zn ions, although exposure in the study was at high Zn levels, 50–2000 mg kg<sup>-1</sup>. Zn is well known to be involved in chlorophyll metabolism, being linked to enzyme and protein activities of the chloroplast and photosynthetic systems.<sup>3,7</sup> The current findings, demonstrate that coating of urea with the dual-capped products does not negate the role of Zn in chlorophyll production.

In line with the early SPAD data, shoot biomass growth was enhanced by all of the Zn-NP-urea nanofertilizers, with the NAC-SAL-Zn and SAL-urea-Zn rate-1 treatments resulting in significantly greater shoot biomass, relative to the control. However, grain biomass yield was similarly affected by all treatments (Fig. 5B). These findings suggest that the products may be targeted more at shoot production and thus would be particularly beneficial in vegetable crop production for human consumption, or forage for animal feed. These assumptions warrant further evaluation in vegetable and forage crops.

### Effect of Zn NP-urea nanofertilizers on nutrient accumulation by sorghum

Grain Zn accumulation and total above-ground (grain + shoot) Zn accumulation were generally similar across all treatments, except for NAC-urea-Zn at rate 2 which significantly promoted grain Zn translocation compared to the SAL-urea-Zn rate-1 by 47%, and total above-ground Zn accumulation by 63% and 64% respectively, compared to NAC-SAL-Zn rate-1 and NAC-urea-Zn rate-1 (Fig. 5C). This finding demonstrates that a lower rate of Zn can be used for this product to deliver adequate Zn comparable to higher doses from other products to fortify both sorghum grain or shoot with Zn, for human or animal nutrition. This confirms our recent report from a study devoid of dual-capping of the nanoscale Zn that coating urea with ZnO NPs can allow for using less Zn in fertilizers, without any penalty on Zn delivery, compared to higher Zn rates.<sup>19</sup> Moreover, the fact that the control treatment composed of a more readily bioavailable Zn species (ions) did not result in a significantly different amount of Zn in the plant tissues than the nano formulations indicates that the coating was effective for delivering Zn. Therefore, whether by facile techniques, such as using water or vegetable oil as a binding agent,<sup>17–19</sup> or by more sophisticated approaches, such as with dual-capped Zn nanoparticles, coating Zn onto urea represents an effective strategy to circumvent the previously described constraints to the application of nanoscale micronutrients in plant fertilization. Notably, it has been shown that nano-scale Zn can enhance the

Zn contents in the aleurone layer, grain crease, and endosperm of wheat grains.<sup>51</sup> By implication, the delivery of Zn into plants using agronomic fortification and the successful translocation of the Zn to edible portions of plants as demonstrated in the current study holds strong promise to address widespread Zn deficiency in plants, animals and humans. However, the chemical nature of Zn in edible plant tissue often reported to be present in the form of Zn-phosphate (see for *e.g.*, ref. 51), a largely nutritionally non-bioavailable Zn form, warrants further studies to understand the nature of the Zn in the tissue from novel nano delivery strategies.

In the case of N, grain N accumulation and total above-ground N accumulation were also generally similar across all nanofertilizer treatments, compared to the control. However, the NAC-urea-Zn rate-2 treatment significantly promoted grain N translocation, relative to the NAC-SAL-Zn rate-1, SAL-urea-Zn rate-1, and NAC-SAL-Zn rate-2 treatments. Also, NAC-urea-Zn rate-2 increased total above-ground N accumulation than did NAC-SAL-Zn rate-1, SAL-urea-Zn rate-1, and NAC-SAL-Zn rate-2 (Fig. 5D). It is worth noting that the nanofertilizer produced with Zn-NPs capped with urea contained a higher amount of N by default (see materials and methods); however, that fact did not necessarily translate into higher plant N in the case of NAC-urea-Zn rate-1 and SAL-urea-Zn rate-1. This suggests that a lower rate of Zn used in the NAC-urea-Zn (namely, rate-2) can facilitate N accumulation. Previously, we reported that Zn enhanced total N uptake in sorghum, compared to treatments lacking Zn, whereby at 6 mg kg<sup>-1</sup>, Zn sulfate resulted in higher total N uptake than ZnO NPs.<sup>52</sup> Similarly, under drought stress, N accumulation was inhibited; however, ZnO NPs at 5 mg kg<sup>-1</sup> restored sorghum above-ground N to levels obtained under sufficient water supply. Notably, the Zn products were separately administered from urea in the study.<sup>52</sup> Contrary to sorghum, Zn did not influence N uptake in wheat, irrespective of whether coated or not onto urea,<sup>19,31</sup> indicating a possible species-dependent response. With P, there was no effect of Zn treatment on grain and total above ground P, irrespective of the Zn type (Fig. 5E). A concentration-dependent interaction of P and Zn in soil that results in the formation of insoluble Zn phosphate can limit the uptake of either or both elements by plants.<sup>53–55</sup> This knowledge led us to evaluate the effect of the urea-Zn nanofertilizers on P uptake by the sorghum plants. Our data indicate that coating of urea with these products does not influence the Zn-P interaction, and hence, P uptake, any more than the conventional Zn sulfate.

### Effect of Zn NP-urea nanofertilizers on soil residual Zn, N and P

Total residual Zn in the soil after growth and harvest of sorghum was highest in the NAC-SAL Zn rate-1 treatment, which was significantly different than the Zn content of the control soil, and those of the NAC-SAL Zn rate-2 and NAC-urea Zn rate-2 treatments (Table 2). In general, there was a trend for more Zn in the soil treated with the nanofertilizers at rate-1, suggesting that these products can better retain Zn in soil,



**Table 2** Effect of Zn–urea nanofertilizers on residual contents of zinc, nitrogen (separately as ammonium and nitrate), and phosphorus in the experimental soil. Values ( $\text{mg kg}^{-1}$ ) are means and SDs and values followed by different letters are significantly different at  $P \leq 0.05$ , separately for Zn, ammonium, nitrate and P ( $n = 3$ )

Treatment	Zn	$\text{NH}_4\text{-N}$	$\text{NO}_3\text{-N}$	P
$\text{ZnSO}_4$ (control)	$1.02 \pm 0.14\text{bc}$	$1.8 \pm 0.22\text{a}$	$0.23 \pm 0.02\text{a}$	$7.73 \pm 1.51\text{b}$
NAC–SAL Zn rate-1	$2.21 \pm 1.02\text{a}$	$1.45 \pm 0.11\text{b}$	$0.24 \pm 0.03\text{a}$	$11.73 \pm 5.06\text{ab}$
NAC–urea Zn rate-1	$1.43 \pm 0.79\text{ab}$	$1.46 \pm 0.06\text{b}$	$0.26 \pm 0.02\text{a}$	$12.53 \pm 1.40\text{ab}$
SAL–urea Zn rate-1	$1.98 \pm 0.47\text{ab}$	$1.15 \pm 0.02\text{b}$	$0.36 \pm 0.18\text{a}$	$14.00 \pm 4.92\text{a}$
NAC–SAL Zn rate-2	$0.32 \pm 0.04\text{c}$	$1.61 \pm 0.05\text{ab}$	$0.24 \pm 0.03\text{a}$	$7.73 \pm 1.51\text{b}$
NAC–urea Zn rate-2	$0.58 \pm 0.15\text{c}$	$1.68 \pm 0.21\text{ab}$	$0.26 \pm 0.03\text{a}$	$8.13 \pm 0.83\text{ab}$

than the control  $\text{ZnSO}_4$ . These data agree with the report of Baddar *et al.*,<sup>56</sup> in which the total soil concentrations of Zn at pH 6 were higher with negatively- and positively charged ZnO nano formulations than with  $\text{ZnSO}_4$ . In the case of N, residual total nutrient was determined as the two fractions in which N exists in soil, namely, ammonium and nitrate. Soil ammonium–N ( $\text{NH}_4\text{-N}$ ) content was significantly higher in the control treatment, compared to all other treatments, with the exception of NAC–urea Zn rate-2 treatment, which showed a median value, compared to other treatments. In contrast to  $\text{NH}_4\text{-N}$ , none of the Zn treatments altered the residual level of nitrate–N ( $\text{NO}_3\text{-N}$ ) in the soil (Table 2). Previous studies indicate that  $\text{ZnSO}_4$  can be used to regulate the process of urea–N transformation to nitrate by acting as both a urease and a nitrification inhibitor.<sup>57,58</sup> This effect leads potentially to more ammonium being retained in the soil. These aspects were not investigated in the present study, although it is tempting to postulate that the control, and to a lesser extent NAC–urea Zn rate-2, promoted ammonium retention possibly due to these effects. For P, residual content was significantly higher in the SAL–urea Zn rate-1 treatment, relative to the control and NAC–SAL Zn rate-2 treatments. Other treatments were of median value, compared to those (Table 2). Coincident with the residual Zn, the trend for

higher (albeit not significant in all cases) residual soil P in the nanofertilizers with a higher Zn rate is also notable. In particular, data with the SAL–urea Zn rate-1 treatment indicate that in soil with high P leachability, this product has the potential to increase P fixation in soil, ostensibly as Zn phosphate.<sup>59</sup> Increased P fixation due to the interaction with metals such as Zn could have implications for lowering P leaching, which could avail soil of more P in the subsequent cropping season, and thereby lower future P application. However, a potential trade-off could be reduced Zn availability. These aspects are topics of ongoing investigation.

## Conclusions

In this study, we report the development of novel nano-enabled fertilizers based on dual capping of Zn nanoparticles with NAC and SAL, and the formulation of urea with the same *via* surface coating. The nanofertilizers showed the potential to maintain plant performance, deliver nutrients to plants and retain nutrients in soil to comparable, if not better, extents to the conventional Zn-sulfate fertilizer. A schematic representation of the synthesis of dual-capped Zn nanoparticles, the functionalization of urea granules with the nanoformulations, and application of the Zn–urea nanofertilizers on wheat to understand their agronomic performance is shown in Fig. 6. The nanoscale Zn species in the formulation was identified to be  $\text{Zn}(\text{OH})_2$ . Given that  $\text{Zn}(\text{OH})_2$  ( $7.8 \times 10^{-4} \text{ mol dm}^{-3}$ ) is more soluble than  $\text{ZnO}$  ( $7.75 \times 10^{-5} \text{ mol dm}^{-3}$ ), the generally similar effects on plants as the conventional Zn-sulfate are not surprising. Coating of urea granules with Zn-NPs capped with the stabilizing agents resulted in comparable, and in several instances better, effects on plant performance, plant delivery and soil retention of Zn, N and P to Zn-sulfate under normal growth conditions. In particular, the rate-2 NAC–urea–Zn treatment indicated the potential of achieving grain Zn fortification for human health using a lower Zn rate. This is important, considering widespread human Zn deficiency and the concern about the sustainability of Zn resources mentioned in the introduction. From a practical standpoint, coating of Zn onto urea permitted achieving the important goal of applying nanoscale Zn in the same fertilization regimen as urea, thereby precluding the need for multiple fertilization events, separately for N and Zn. Furthermore, by itself, Zn is effective in alleviating environmental stresses in plants, as demonstrated by several of our previous studies.<sup>19,47</sup> Based on the above-described

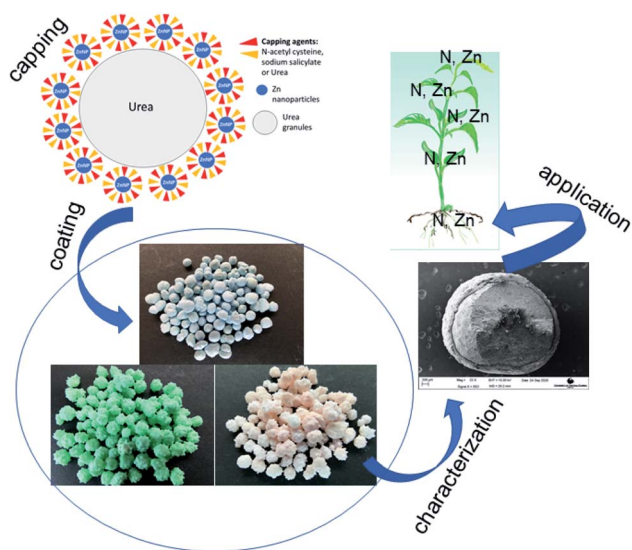


**Fig. 6** Schematic depiction of the synthesis of dual-capped Zn nanoparticles, functionalization of urea granules with the capped nano formulations, and evaluation of the nanofertilizer products in plant.



biological effects of the capping agents and Zn, it is highly likely that the observed effects of the nanofertilizers on plant performance and nutrient delivery will be escalated under adverse environmental conditions such as drought and disease infestation, wherein plant productivity and nutrient acquisition are negatively impacted. Research is currently ongoing to assess the potential of these products on crop performance and nutrient fortification under disease and abiotic stress conditions.

The question of cost-effectiveness often arises with novel agrochemical formulations and needs to be evaluated. Nano-scale products are presumed expensive initially simply because their manufacture is an add-on to an existing process or product. However, subsequent validation of their enhanced effects on crop performance over conventional products, especially when used at lower rates, is a potential cost-saving outcome for both the farmer and the environment. Moreover, scaling up the nano production process should bring about a reduction in the cost of production, and consequently, the cost of nano inputs.

## Author contributions

Christian Dimkpa, Upendra Singh, and Swadeshmukul Santra conceived the research.

Maria Campos, Ali Ozcan, and Ziyang Huang conducted nano synthesis, capping and characterization of the finished product.

Job Fugice and Katherine Glass performed urea coating with the nanoformulations.

Katherine Glass, Job Fugice and Christian Dimkpa performed plant studies and analysis of nutrient content in plant and soil.

Christian Dimkpa and Maria Campos wrote the draft manuscript.

Christian Dimkpa, Maria Campos, Upendra Singh, and Swadeshmukul Santra revised the manuscript.

## Conflicts of interest

There is no conflict of interest for this research.

## Acknowledgements

This work was funded by the United States Agency for International Development (USAID) through the Feed the Future Soil Fertility Technology Adoption, Policy Reform and Knowledge Management Project Cooperative Agreement (Number AID-BFS-IO-15-00001) with the International Fertilizer Development Center. The authors acknowledge the UCF Materials Innovation for Sustainable Agriculture Center for facilities and technical support.

## References

1 C. O. Dimkpa and P. S. Bindraban, Micronutrients fortification for efficient agronomic production *Agron. Sustainable Dev.*, 2016, **36**, 1–26.

- 2 D. L. Jones, P. Cross, P. J. A. Withers, T. H. DeLuca, D. A. Robinson, R. S. Quilliam, I. M. Harris, D. R. Chadwick and G. Edwards-Jones, Review: Nutrient stripping: the global disparity between food security and soil nutrient stocks, *J. Appl. Ecol.*, 2013, **50**, 851–862.
- 3 C. Noulas, M. Tziouvalekas and T. Karyotis, Zinc in soils, water and food crops, *J. Trace Elem. Med. Biol.*, 2018, **49**, 252–260.
- 4 D. Montalvo, F. Degryse, R. C. da Silva R. Baird and M. J. McLaughlin, Agronomic effectiveness of zinc sources as micronutrient fertilizer, in *Advances in Agronomy*, ed. D. L. Sparks, Elsevier Academic Press Inc, San Diego, 2016, pp. 215–267.
- 5 L. Abeywardana, M. de Silva, C. Sandaruwan, D. Dahanayake, G. Priyadarshana, S. Chathurika, V. Karunaratne and N. Kottegoda, Zinc-doped hydroxyapatite-urea nanoseed coating as an efficient macro-micro plant nutrient delivery agent, *ACS Agric. Sci. Technol.*, 2021, **1**, 230–239.
- 6 C. Dimkpa and P. Bindraban, Nanofertilizers: new products for the industry?, *J. Agric. Food Chem.*, 2018, **66**, 6462–6473.
- 7 T. C. Thounaojam, T. T. Meetei, Y. B. Devi, S. K. Panda and H. Upadhyaya, Zinc oxide nanoparticles (ZnO-NPs): a promising nanoparticle in renovating plant science, *Acta Physiol. Plant.*, 2021, **43**, 136.
- 8 R. Raliya, V. Saharan, C. Dimkpa and P. Biswas, Nanofertilizer for precision and sustainable agriculture: current state and future perspectives, *J. Agric. Food Chem.*, 2018, **66**, 6487–6503.
- 9 F. Piccinno, F. Gottschalk, S. Seeger and B. Nowack, Industrial production quantities and uses of ten engineered nanomaterials in Europe and the world, *J. Nanopart. Res.*, 2012, **14**, 1109.
- 10 M. Kah, R. S. Kookana, A. Gogos and T. D. Bucheli, A critical evaluation of nanopesticides and nanofertilizers against their conventional analogues, *Nat. Nanotechnol.*, 2018, **13**, 677–684.
- 11 I. O. Adisa, V. L. R. Pullagurala, J. R. Peralta-Videa, C. O. Dimkpa, W. H. Elmer, J. L. Gardea-Torresdey and J. C. White, Recent advances in nano-enabled fertilizers and pesticides: A critical review of mechanisms of action, *Environ. Sci.: Nano*, 2019, **6**, 2002–2030.
- 12 W. Elmer and J. C. White, The future of nanotechnology in plant pathology, *Annu. Rev. Phytopathol.*, 2018, **56**, 111–133.
- 13 J. C. White and J. L. Gardea-Torresdey, Achieving food security through the very small, *Nat. Nanotechnol.*, 2018, **13**, 627–629.
- 14 C. García-Gómez, A. Obrador, D. González, M. Babin and M. D. Fernández, Comparative effect of ZnO NPs, ZnO bulk and ZnSO<sub>4</sub> in the antioxidant defences of two plant species growing in two agricultural soils under greenhouse conditions, *Sci. Total Environ.*, 2017, **589**, 11–24.
- 15 H. Qiu and E. Smolders, Nanospecific phytotoxicity of CuO nanoparticles in soils disappeared when bioavailability factors were considered, *Environ. Sci. Technol.*, 2017, **51**, 11976–11985.



- 16 G. A. Santos, G. H. Korndorfer, H. S. Pereira and W. Paye, Addition of micronutrients to NPK formulation and initial development of maize plants, *Biosci. J.*, 2018, **34**, 927–936.
- 17 N. Milani, M. J. McLaughlin, S. P. Stacey, J. K. Kirby, G. M. Hettiarachchi, D. G. Beak and G. Cornelis, Dissolution kinetics of macronutrient fertilizers coated with manufactured zinc oxide nanoparticles, *J. Agric. Food Chem.*, 2012, **60**, 3991–3998.
- 18 N. Milani, G. M. Hettiarachchi, J. K. Kirby, D. G. Beak, S. P. Stacey and M. J. McLaughlin, Fate of zinc oxide nanoparticles coated onto macronutrient fertilizers in an alkaline calcareous soil, *PLoS One*, 2015, **10**, e0126275.
- 19 C. O. Dimkpa, J. Andrews, J. Fugice, U. Singh, P. S. Bindraban, W. H. Elmer, J. L. Gardea-Torresdey and J. C. White, Facile coating of urea with low-dose ZnO nanoparticles promotes wheat performance and enhances Zn uptake under drought stress, *Front. Plant Sci.*, 2020, **11**, 168.
- 20 C. O. Dimkpa, J. Fugice, U. Singh and T. Lewis, Development of fertilizers for enhanced nitrogen use efficiency – trends and perspectives, *Sci. Total Environ.*, 2020, **731**, 139113.
- 21 *Nanotechnologies in Food and Agriculture*, ed. M. Rai, C. Ribeiro, L. Mattoso and N. Duran. Springer Publishers, 2015, p. 352.
- 22 D. K. Ghosh, S. Kokane, P. Kumar, A. Ozcan, A. Warghane, M. Motghare, S. Santra and A. K. Sharma, Antimicrobial nano-zinc oxide-2S albumin protein formulation significantly inhibits growth of “candidatus *Liberibacter asiaticus*” in planta, *PLoS One*, 2018, **13**, e0204702.
- 23 G. A. Goldstein, N-acetylcysteine amide (nac amide) for enhancing plant resistance and tolerance to environmental stress, *US Pat.*, WO2006132712A2, 2006.
- 24 M. Nozulaidi, M. S. Jahan, M. Khairi, M. M. Khandaker, M. Nashriyah and Y. M. Khanif, N-acetylcysteine increased rice yield, *Turk. J. Agric. For.*, 2015, **39**, 204–211.
- 25 L. S. Muranaka, T. E. Giorgiano, M. A. Takita, M. R. Forim, L. F. C. Silva, H. D. Coletta-Filho, M. A. Machado and A. A. de Souza, N-Acetylcysteine in agriculture, a novel use for an old molecule: focus on controlling the plant-pathogen *Xylella fastidiosa*, *PLoS One*, 2013, **8**, e72937.
- 26 N. Munirah, M. S. Jahan and M. Nashriyah, N-acetylcysteine and Zn regulate corn yield, *ScienceAsia*, 2015, **41**, 246–250.
- 27 N. Syuhada and M. S. Jahan, Glutathione functions on physiological characters to increase copper-induced corn production, *Russ Agr. Sci.*, 2016, **42**, 5–10.
- 28 Y. M. Koo, A. Y. Heo and H. W. Choi, Salicylic acid as a safe plant protector and growth regulator, *Plant Pathol. J.*, 2020, **36**, 1–10.
- 29 M. R. Sofy, Application of salicylic acid and zinc improves wheat yield through physiological processes under different levels of irrigation intervals, *Int. J. Plant Res.*, 2015, **5**, 136–156.
- 30 A. A. El-Yazied, Effect of foliar application of salicylic acid and chelated zinc on growth and productivity of sweet pepper (*Capsicum annuum* L.) under Autumn planting, *Res. J. Agric. Biol. Sci.*, 2011, **7**, 423–433.
- 31 C. O. Dimkpa, J. Andrews, J. Sanabria, P. S. Bindraban, U. Singh, W. H. Elmer, J. L. Gardea-Torresdey and J. C. White, Interactive effects of drought, organic fertilizer, and zinc oxide nanoscale and bulk particles on wheat performance and grain nutrient accumulation, *Sci. Total Environ.*, 2020, **722**, 137808.
- 32 R. G. Menon, S. H. Chien and W. J. Chardon, Iron oxide-impregnated filter paper (Pi test): II. A review of its application, *Nutr. Cycling Agroecosyst.*, 1996, **47**, 7–18.
- 33 National Center for Biotechnology Information, *PubChem Compound Summary for CID 12035, Acetylcysteine*, retrieved Oct 30, 2020, <https://pubchem.ncbi.nlm.nih.gov/compound/Acetylcysteine>.
- 34 C. O. Dimkpa, A. Calder, J. E. McLean, D. W. Britt and A. J. Anderson, Responses of a soil bacterium, *Pseudomonas chlororaphis* O6 to commercial metal oxide nanoparticles compared with responses to metal ions, *Environ. Pollut.*, 2011, **159**, 1749–1756.
- 35 N. Martineau, J. E. McLean, C. O. Dimkpa, D. W. Britt and A. J. Anderson, Components from wheat roots modify the bioactivity of ZnO and CuO nanoparticles in a soil bacterium, *Environ. Pollut.*, 2014, **187**, 65–72.
- 36 R. Marsalek, Particle size and zeta potential of ZnO, *APCBEE Proc.*, 2014, **9**, 13–17.
- 37 J. Jiang, G. Oberdorster and P. Biswas, Characterization of size, surface charge, and agglomeration state of nanoparticle dispersions for toxicological studies, *J. Nanopart. Res.*, 2009, **11**, 77–89.
- 38 A. M. El badawy, T. P. Luxton, R. G. Silva, K. G. Scheckel, M. T. Suidan and T. M. Tolaymat, Impact of environmental conditions (pH, ionic strength, and electrolyte type) on the surface charge and aggregation of silver nanoparticles suspensions, *Environ. Sci. Technol.*, 2010, **44**, 1260–1266.
- 39 C. O. Dimkpa, Soil properties influence the response of terrestrial plants to metallic nanoparticles exposure, *Curr. Opin. Environ. Sci. Health*, 2018, **6**, 1–8.
- 40 M. Picquart, Z. Abedinzadeh, L. Grajcar and M. H. Baron, Spectroscopic study of N-acetylcysteine and N-acetylcystine/hydrogen peroxide complexation, *Chem. Phys.*, 1998, **228**, 279–291.
- 41 T. B. Rawal, M. D. Smith, A. Ozcan, J. C. Smith, L. Tetard, S. Santra and L. Petridis, Role of capping agents in the synthesis of salicylate-capped zinc oxide nanoparticles, *ACS Appl. Nano Mater.*, 2020, **3**, 9951–9960.
- 42 M. Manivannan and S. Rajendran, Investigation of inhibitive action of urea-Zn<sup>2+</sup> system in the corrosion control of carbon steel in sea water, *Int. J. Eng. Res. Sci. Technol.*, 2011, **3**, 8048–8060.
- 43 D. Philip, A. John, C. Y. Panicker and H. T. Varghese, FT-Raman, FT-IR and surface enhanced Raman scattering spectra of sodium salicylate, *Spectrochim. Acta, Part A*, 2001, **57**, 1561–1566.
- 44 G. Aldini, A. Altomare, G. Baron, G. Vistoli, M. Carini, L. Borsani and F. Sergio, N-Acetylcysteine as an antioxidant and disulphide breaking agent: the reasons why, *Free Radical Res.*, 2018, **52**, 751–762.



- 45 O. B. Ibrahim, M. S. Refat, M. Salman and M. M. AL-Majthoub, Chemical Studies on the uses of urea complexes to synthesize compounds having electrical and biological applications, *Int. J. Mater. Sci.*, 2012, **2**, 67–82.
- 46 F. C. Silva, L. C. B. Lima, C. Viseras, J. A. Osajima, J. M. da Silva Júnior, R. L. Oliveira, L. R. Bezerra and E. C. Silva-Filho, Understanding urea encapsulation in different clay minerals as a possible system for ruminant nutrition, *Molecules*, 2019, **24**, 3525.
- 47 A. Ulusal and C. Avsar, Understanding caking phenomena in industrial fertilizers, *Chem. Biochem. Eng. Q.*, 2020, **34**, 209–222.
- 48 M. Irfan, M. B. K. Niazi, A. Hussain, W. Farooq and M. H. Zia, Synthesis and characterization of zinc-coated urea fertilizer, *J. Plant Nutr.*, 2018, **41**, 1625–1635.
- 49 C. O. Dimkpa, J. C. White, W. H. Elmer and J. Gardea-Torresdey, Nanoparticle and ionic Zn promote nutrient loading of sorghum grain under low NPK fertilization, *J. Agric. Food Chem.*, 2017, **65**, 8552–8559.
- 50 L. V. Subbaiah, T. N. V. K. V. Prasad, T. G. Krishna, P. Sudhakar, B. R. Reddy and T. Pradeep, Novel effects of nanoparticulate delivery of zinc on growth, productivity, and zinc biofortification in maize (*Zea mays* L.), *J. Agric. Food Chem.*, 2016, **64**, 3778–3788.
- 51 T. Zhang, H. Sun, Z. Lv, L. Cui, H. Mao and P. M. Kopittke, Using synchrotron-based approaches to examine the foliar application of ZnSO<sub>4</sub> and ZnO nanoparticles for field-grown winter wheat, *J. Agric. Food Chem.*, 2018, **66**, 2572–2579.
- 52 C. O. Dimkpa, U. Singh, P. S. Bindraban, W. H. Elmer, J. L. Gardea-Torresdey and J. C. White, Zinc oxide nanoparticles alleviate drought-induced alterations in sorghum performance, nutrient acquisition, and grain fortification, *Sci. Total Environ.*, 2019, **688**, 926–934.
- 53 X. D. Cao, A. Wahbi, L. N. Ma, B. Li and Y. L. Yang, Immobilization of Zn, Cu, and Pb in contaminated soils using phosphate rock and phosphoric acid, *J. Hazard. Mater.*, 2009, **164**, 555–564.
- 54 S. J. Watts-Williams and T. R. Cavagnaro, Arbuscular mycorrhizas modify tomato responses to soil zinc and phosphorus addition, *Biol. Fertil. Soils*, 2012, **48**, 285–294.
- 55 M. Andrunik, M. Wołowiec, D. Wojnarski, S. Sylwia Zelek-Pogudz and T. Bajda, Transformation of Pb, Cd, and Zn minerals using phosphates, *Minerals*, 2020, **10**, 342.
- 56 E. Z. Baddar, C. J. Matocha and J. M. Unrine, Surface coating effects on the sorption and dissolution of ZnO nanoparticles in soil, *Environ. Sci.: Nano*, 2019, **6**, 2495–2507.
- 57 R. B. A. Khariri, M. K. Yusop, M. H. Musa and A. Hussin, Laboratory evaluation of metal elements urease inhibitor and DMPP nitrification inhibitor on nitrogenous gas losses in selected rice soils, *Water, Air, Soil Pollut.*, 2016, **227**, 232.
- 58 M. Montoya, A. Castellano-Hinojosa, A. Vallejo, J. M. Álvarez, E. J. Bedmar, J. Recio and G. Guardia, Zinc fertilizers influence greenhouse gas emissions and nitrifying and denitrifying communities in a non-irrigated arable cropland, *Geoderma*, 2018, **325**, 208–217.
- 59 J. Lv, S. Zhang, L. Luo, W. Han, J. Zhang, K. Yang and P. Christie, Dissolution and microstructural transformation of ZnO nanoparticles under the influence of phosphate, *Environ. Sci. Technol.*, 2012, **46**, 7215–7221.

